

CrossMark  
click for updatesCite this: *RSC Adv.*, 2014, 4, 59831Received 24th October 2014  
Accepted 4th November 2014

DOI: 10.1039/c4ra13103g

www.rsc.org/advances

## Desorption-controlled separation of natural gas alkanes by zeolite membranes†

R. Dragomirova,<sup>a</sup> M. Stöhr,<sup>a</sup> C. Hecker,<sup>b</sup> U. Lubenau,<sup>c</sup> D. Paschek<sup>d</sup> and S. Wohlrab<sup>\*a</sup>

The performance of porous membranes is tremendously influenced by desorption, as alkane separations by a pressure stable MFI membrane revealed. High membrane selectivities as well as permeation fluxes are to be traced back to the fact that a reduced permeate pressure significantly decreases the loading gradient of the adsorbed molecules in the membrane.

With regard to the continuing demand on carbon feedstocks, C<sub>2–5</sub> alkanes from natural gas possess tremendous potential.<sup>1–6</sup> In addition to catalytic alkane conversions, the substitution of present separation technologies for natural gas alkanes by low energetic alternatives<sup>7–9</sup> would be the essential economic progress for their increased use in the chemical industry. In this context, membranes based on silicon rubber have currently found practical application.<sup>7</sup> However, with typical mixed-gas propane/methane selectivities of 3–5 and butane/methane selectivities of 5–10 they are preferably used for natural gas processing. Higher selectivities are necessary for targeted alkane isolation and were reported for more advanced polymer membranes.<sup>10</sup> Even so, heavy hydrocarbons cause swelling of polymer membranes, leading to increased permeation for all components and a decrease of the separation ability over time.<sup>11</sup> So far, non-swellable zeolite membranes were not applicable since they lost in direct competition with polymer membranes in terms of selectivity. However, due to their specific properties, such as a well-defined pore system, pressure and thermal

stability as well as their non-swellability zeolite membranes should be an alternative in the application of selective membrane separation processes.<sup>12,13</sup>

The understanding of the underlying interactions between zeolite membrane and adsorbed molecules is the key for a successful application. A five-step transport model has been proposed for adsorption driven zeolite membrane separation including: (1) adsorption at the external surface; (2) transport from the external surface into the pores; (3) intracrystalline transport; (4) transport from the pores to the external surface and (5) desorption from the external surface.<sup>14,15</sup> Xiao and Wei differentiate between activated gas transport and surface diffusion during intracrystalline diffusion in microporous materials.<sup>16</sup> According to van de Graaf the permeation flux through the zeolite membrane by surface diffusion can be expressed by eqn (1).<sup>17</sup>

$$N_i^s = D_i^s \rho q_{\text{sat},i} \nabla \ln(1 - \theta_i) \quad \text{with} \quad D_i^s = D_i^{s,0} \exp\left\{\frac{-E_a}{RT}\right\} \quad (1)$$

$N_i^s$  is the flux of the component  $i$  in [mol m<sup>-2</sup> s<sup>-1</sup>] and  $D_i^s$  is the diffusivity of component  $i$  in [m<sup>2</sup> s<sup>-1</sup>];  $q_{\text{sat},i}$  and  $\theta_i$  represent the saturation concentration in the zeolite in [mol g<sup>-1</sup>] and the occupancy in the membrane, respectively;  $\rho$  is the material density in [g m<sup>-3</sup>].

Additional to differences in occupancy/loading of components, a preferential adsorption of one component hinders the permeation of the other one leading to higher separation selectivities.<sup>18</sup> For example, the preferential enrichment of a higher alkane from mixtures consisting of methane/ethane or ethane/isobutene was reported for silicalite-1 and composite alumina-MFI zeolite membranes, respectively.<sup>19,20</sup> Thus, the operating parameters – pressure and temperature – are considered to be the important control variables influencing the membrane performance.<sup>15,19</sup> The temperature essential to achieve the maximum permeation flux of a single component through the membrane increases with the adsorption strength of the molecule.<sup>21,22</sup> The positive influence of an increased

<sup>a</sup>Leibniz Institute for Catalysis, University of Rostock, Albert-Einstein-Str. 29a, D-18059 Rostock, Germany. E-mail: sebastian.wohrlab@catalysis.de

<sup>b</sup>Technical University Freiberg, Institute for Electronic and Sensor Materials, Gustav-Zeuner-Str. 3, D-09599 Freiberg, Germany

<sup>c</sup>DBI Gas-und Umwelttechnik GmbH, Karl-Heine Straße 109/111, D-04229 Leipzig, Germany

<sup>d</sup>Institute für Chemie, Abteilung Physikalische Chemie, Universität Rostock, Dr-Lorenz-Weg 1, D-18059 Rostock, Germany

† Electronic supplementary information (ESI) available: Membrane preparation and characterization by permoporometry; calculated single gas adsorption isotherms, permeation flux calculation and determination; mixed gas adsorption isotherms and separation experiments. See DOI: 10.1039/c4ra13103g



pressure difference on the permeation flux through MFI membranes of *n*-butane single gas was already described by Gump *et al.*<sup>23</sup> With regard to the separation of alkanes, the principal applicability of MFI membranes could already have been demonstrated.<sup>24,25</sup> Recently, we showed that by increasing the feed pressure, a higher *n*-butane adsorption/condensation probability at the membrane surface could be achieved, hindering methane to permeate and thus improving the separation selectivity.<sup>25–27</sup> While the impact of diffusion and adsorption on zeolite membranes became clear, it was still not effective enough to reach polymer membrane performances.

For this work we used pressure stable nearly defect-free MFI-membranes (Fig. S1, ESI†) with a Si/Al ratio of 270 and layer thicknesses of approximately 40  $\mu\text{m}$  on inert  $\alpha\text{-Al}_2\text{O}_3$  supports prepared by a two-step synthesis process.<sup>25</sup> The customized MFI membranes (effective surface area =  $22 \times 10^{-4} \text{ m}^2$ ) equipped with a MFI sublayer acting as mechanical stabilizer were used in single and mixed gas permeation experiments with methane and *n*-butane. The separation ability of the membrane is characterized by the so called separation factor – the molar ratio of *n*-butane over methane in the permeate divided by the molar ratio of *n*-butane over methane in the retentate. From configurational biased Monte Carlo (CBMC) simulations realistic adsorption isotherms for single as well mixed gases were computed as previously reported.<sup>27</sup>

Calculated single gas adsorption isotherms of 100 vol% methane and 100 vol% *n*-butane, respectively, locate the loading of both components and the mechanism of the intracrystalline diffusion in such a membrane therewith (Fig. S2, ESI†). The low loading of methane and high loading of *n*-butane at the feed and the permeate side of a MFI membrane under operating conditions are illustrated in Fig. 1a. At increasing temperatures – from 293 to 348 K – a more pronounced decline in the loading of methane at the feed side is obvious, whereas temperature variation changes the feed loading of *n*-butane less. At lower permeate pressure and increased temperature the loading of *n*-butane at the permeate side is significantly decreased, while nearly no methane molecule is adsorbed below 0.05 bar. The significance of the loading on the permeation flux across the MFI membrane can be conjectured from a series of single gas permeation measurements accomplished at different temperatures with both, methane and *n*-butane (Fig. 1b and c – circles), and the underlying surface diffusion model (1) (Fig. 1b and c – lines).

In the case of methane (Fig. 1b), the loading slope and therewith the flux decreases with increasing temperature, whereas for the case of *n*-butane (Fig. 1c) the flux increases. From Fig. 1b it can be seen that reducing the permeate pressure results in an almost linear increase of the permeation flux for methane. Obviously, the process is quite temperature dependent, where an increase in temperature leads to reduction in permeation flux. At a permeate pressure of 0.01 bar the permeation fluxes are  $2437 \text{ L h}^{-1} \text{ m}^{-2}$  and  $1850 \text{ L h}^{-1} \text{ m}^{-2}$  at 298 and 348 K, respectively. Similar temperature dependence of the permeation fluxes of methane as a function of feed pressure was reported by Burggraaf *et al.*<sup>22</sup> The observed flattening of the experimental permeation flux of methane (Fig. 1b, circles) at

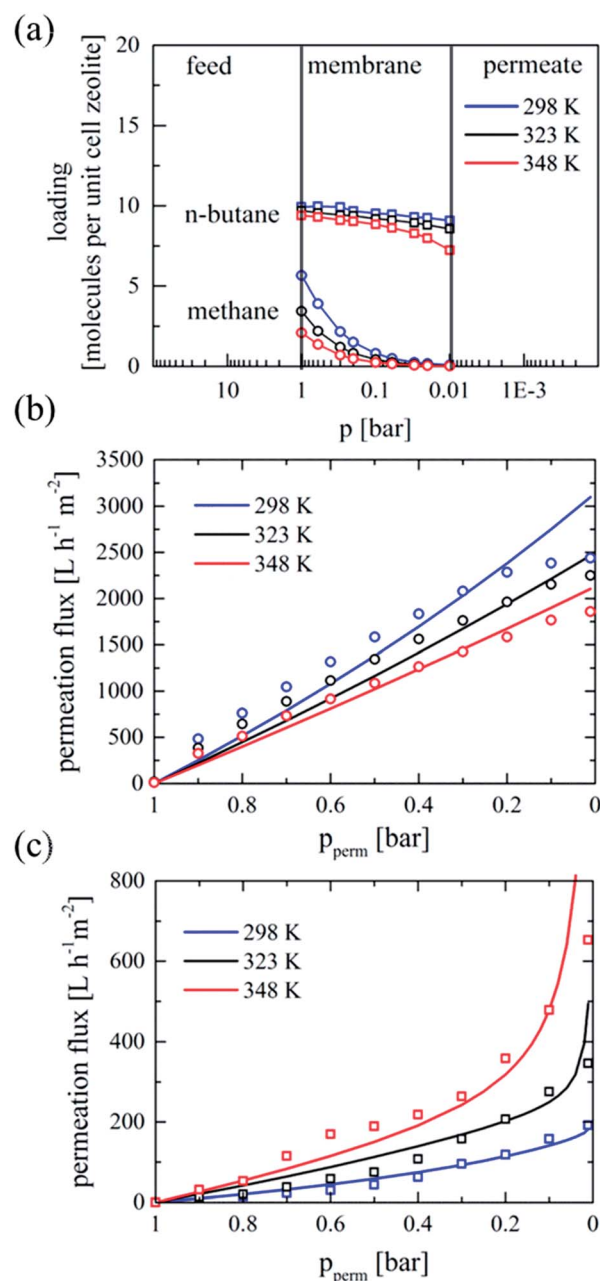


Fig. 1 Single gas permeation of methane and *n*-butane in MFI-membranes, (a) schematic representation of the loading of pure methane and pure *n*-butane at the feed and permeate side, and as guide for the eyes the loading across the membrane calculated from the adsorption isotherms. (b) Experimental permeation fluxes of methane (circles) and predictions of the permeation flux according to the surface diffusion model (lines) at stepwise reduced permeate pressure at feed pressure of 1 bar. (c) See (b) but for *n*-butane.

low permeate pressures is due to the feed streams used. At permeate pressures of approximately 0.2 bar nearly the whole feed stream of methane permeates through the membrane. An increase of the feed flux from  $6 \text{ L h}^{-1}$  to  $12 \text{ L h}^{-1}$  results in a nearly linear increase in permeation (Fig. S3, ESI†). In case of *n*-butane, due to the stronger molecular interactions with the MFI structure smaller overall permeation fluxes were detected



(Fig. 1c, circles). However, the reduced pressure on the permeate side improves apparently the permeation as a consequence of the enhanced surface diffusion caused by the decreased loading of *n*-butane molecules at the permeate side. The increase in the concentration gradient of *n*-butane at lower permeate pressures due to the decreased coverages at the permeate side was described as well by Gump *et al.*<sup>23</sup> In contrast to sweep gas, vacuum reduces the diffusion resistance of the permeating species. Furthermore, a higher mobility of the adsorbed molecules is favoured by the moderate temperature increase and contributes to a higher flux. Additionally, as further experiments (Fig. S4, ESI†) show, increase in the feed pressure to 2 bar gives rise to higher permeation fluxes for *n*-butane which are still exponentially depended on the reduced permeate pressure, whereas the whole feed of methane permeates through the membrane at permeate pressure below 0.8 bar due to the higher pressure difference and the smaller molecule size.

The different permeation characteristics of both alkanes, methane and *n*-butane, at reduced permeate pressures have a significant influence on the separation of both molecules. The calculated mixed gas-adsorption isotherms for a model mixture consisting of 92 vol% methane and 8 vol% *n*-butane reveals the preferable adsorption of *n*-butane in the operating regime (see Fig. S5, ESI†). Schematic representation of the loading at the feed and permeate side is depicted in Fig. 2a. Here, the loading slope of *n*-butane in mixture is more pronounced in comparison to the loading slope of the respective single gas adsorption isotherms. Moreover, an increase in processing temperature leads to even higher change in loading of *n*-butane. For methane a practically negligible small loading in the operating pressure range is obvious.

Arruebo *et al.* had given an indirect evidence on the significance of desorption of the permeating species<sup>24</sup> but experiments failed since pressure stable membranes were not available. Since we use pressure stable membranes<sup>25</sup> we clearly can demonstrate the tremendous influence of desorption on the separation performance. Experiments with the model mixture were conducted at 298 K, 323 K and 348 K, respectively. In this case, the feed pressure was adjusted to 2 bar and a feed flow of 6 L h<sup>-1</sup> was applied. Additionally, separation experiments with feed pressure of 1 bar were conducted (Fig. S6, ESI†). In Fig. 2b and c the permeation fluxes and the development of the separation factors are displayed. By reducing the permeate pressure and thus decreasing the loading of the preferably adsorbed *n*-butane molecules an exponentially improved separation is observed.

The enhanced selectivity could be attributed to the relatively higher permeation flux of *n*-butane as a direct result of the increased mobility due to higher loading gradients between feed and reduced permeate pressure. Moreover, a comparable exponential dependence of the permeation flux as the one observed in the single gas measurements for *n*-butane was found. Furthermore, moderate increase of the temperature intensifies the process and leads to even higher permeation fluxes above 350 L h<sup>-1</sup> m<sup>-2</sup> and excellent separation factors above 60 which are in the range of advanced polymer

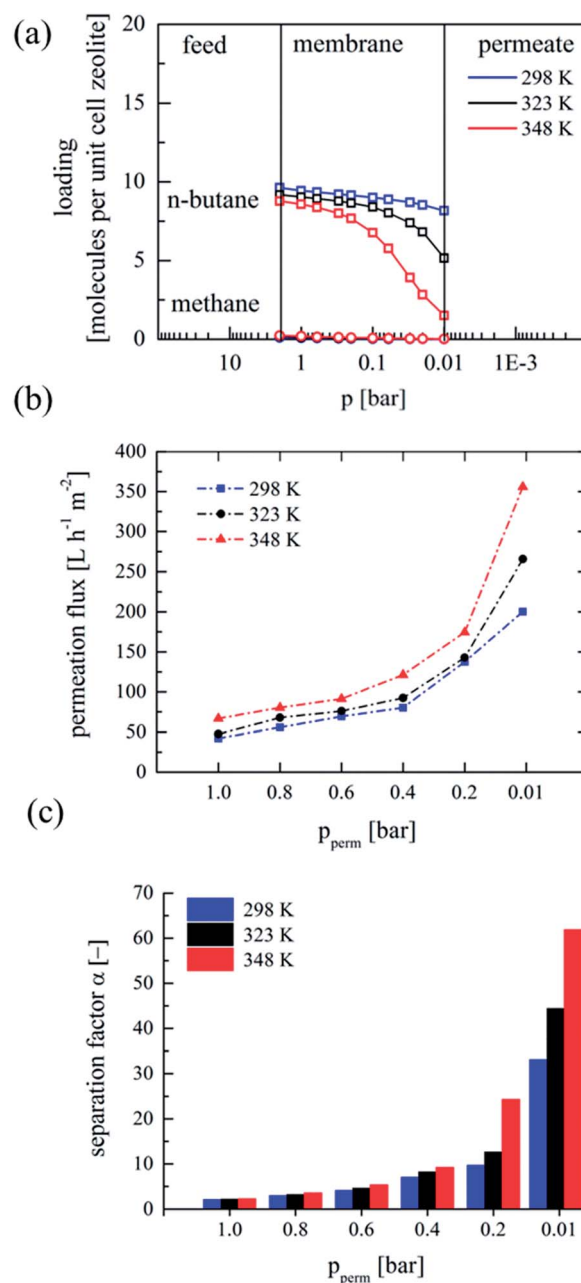


Fig. 2 Mixed gas permeation experiments of mixture comprising 92 vol% methane and 8 vol% *n*-butane, (a) schematic representation of the loading on the feed and permeate side, and as guide for the eyes the loading across the membrane calculated from the adsorption isotherms; (b) permeation fluxes and (c) separation factor  $\alpha_{C_4/C_1}$  at constant feed pressure of 2 bar at stepwise reduced permeate pressure.

membranes.<sup>10</sup> It is obvious that the increase in desorption is directly correlated with the enhanced permeation flux. The increased permeation flux itself is the influencing parameter for the selectivity since more preferably adsorbed *n*-butane permeates across the membrane at lower permeate-pressures.

In conclusion, the impact of desorption on the separation performance of MFI-membranes is evidenced. The enhanced separation is governed to a great extent by the improved



desorption of the mainly adsorbed species, representing a key aspect in the adsorptive separation of natural gas alkanes. Thus, under permeate vacuum inorganic zeolite membranes could be an alternative to polymer membranes for the separation of natural gas alkanes.

## Acknowledgements

Financial support by DFG (within SPP1570) and AiF "Otto von Guericke" e.V. is gratefully acknowledged.

## Notes and references

- 1 M. Baerns and O. Buyevskaya, *Catal. Today*, 1998, **45**, 13–22.
- 2 M. Sun, J. Zhang, P. Putaj, V. Caps, F. Lefebvre, J. Pelletier and J.-M. Basset, *Chem. Rev.*, 2013, **114**, 981–1019.
- 3 F. Cavani, N. Ballarini and A. Cericola, *Catal. Today*, 2007, **127**, 113–131.
- 4 T. Punniyamurthy, S. Velusamy and J. Iqbal, *Chem. Rev.*, 2005, **105**, 2329–2364.
- 5 J. L. Nieto, *Top. Catal.*, 2006, **41**, 3–15.
- 6 J. Brazdil, *Top. Catal.*, 2006, **38**, 289–294.
- 7 R. W. Baker and K. Lokhandwala, *Ind. Eng. Chem. Res.*, 2008, **47**, 2109–2121.
- 8 C. A. Scholes, G. W. Stevens and S. E. Kentish, *Fuel*, 2012, **96**, 15–28.
- 9 P. Bernardo, E. Drioli and G. Golemme, *Ind. Eng. Chem. Res.*, 2009, **48**, 4638–4663.
- 10 Y. Yampolskii, L. Starannikova, N. Belov, M. Bermeshev, M. Gringolts and E. Finkelshtein, *J. Membr. Sci.*, 2014, **453**, 532–545.
- 11 K. Ohlrogge and T. Brinkmann, *Ann. N. Y. Acad. Sci.*, 2003, **984**, 306–317.
- 12 J. Caro and M. Noack, *Microporous Mesoporous Mater.*, 2008, **115**, 215–233.
- 13 A. Tavoraro and E. Drioli, *Adv. Mater.*, 1999, **11**, 975–996.
- 14 R. M. Barrer, *J. Chem. Soc., Faraday Trans.*, 1990, **86**, 1123–1130.
- 15 W. J. W. Bakker, F. Kapteijn, J. Poppe and J. A. Moulijn, *J. Membr. Sci.*, 1996, **117**, 57–78.
- 16 J. Xiao and J. Wei, *Chem. Eng. Sci.*, 1992, **47**, 1123–1141.
- 17 J. M. van de Graaf, F. Kapteijn and J. A. Moulijn, *J. Membr. Sci.*, 1998, **144**, 87–104.
- 18 J. Coronas and J. Santamaría, *Sep. Purif. Methods*, 1999, **28**, 127–177.
- 19 J. M. van de Graaf, E. van der Bijl, A. Stol, F. Kapteijn and J. A. Moulijn, *Ind. Eng. Chem. Res.*, 1998, **37**, 4071–4083.
- 20 M. Jiang, M. Eic, S. Miachon, J.-A. Dalmon and M. Kocirik, *Sep. Purif. Technol.*, 2001, **25**, 287–295.
- 21 W. J. W. Bakker, L. J. P. Van Den Broeke, F. Kapteijn and J. A. Moulijn, *AIChE J.*, 1997, **43**, 2203–2214.
- 22 A. J. Burggraaf, Z. A. E. P. Vroon, K. Keizer and H. Verweij, *J. Membr. Sci.*, 1998, **144**, 77–86.
- 23 C. J. Gump, X. Lin, J. L. Falconer and R. D. Noble, *J. Membr. Sci.*, 2000, **173**, 35–52.
- 24 M. Arruebo, J. Coronas, M. Menéndez and J. Santamaría, *Sep. Purif. Technol.*, 2001, **25**, 275–286.
- 25 S. Wohlrab, T. Meyer, M. Stöhr, C. Hecker, U. Lubenau and A. Oßmann, *J. Membr. Sci.*, 2011, **369**, 96–104.
- 26 K. Neubauer, U. Lubenau, C. Hecker, B. Lücke, D. Paschek and S. Wohlrab, *Chem. Ing. Tech.*, 2013, **85**, 713–722.
- 27 K. Neubauer, R. Dragomirova, M. Stöhr, R. Mothes, U. Lubenau, D. Paschek and S. Wohlrab, *J. Membr. Sci.*, 2014, **453**, 100–107.

